ISSN: 1687-1006 p
ISSN: 2682-3640 e

The Egyptian International Journal of Engineering Sciences and Technology

Vol. 31 (2020) 71–82

https://eijest.journals.ekb.eg/

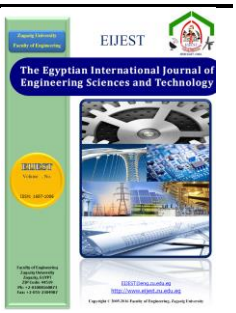

Analysis of homogeneous steady state nanofluid surrounding cylindrical solid pipes

Ahmed S. Rashed*, Tarek A. Mahmoud and Magda M. Kassem

Department of Physics and Engineering Mathematics, Faculty of Engineering Zagazig University, Zagazig 44515, Egypt

ARTICLE INFO

Keywords:

Nanofluids
Nanoparticles
Boundary layer
Flow characteristics
Group method
Similarity solution

ABSTRACT

The current paper is devoted to exploring and investigation of homogeneous steady state nanofluid surrounding cylindrical solid pipes in two dimensions. The modelling system was transformed to a system of ordinary differential equations via the group method of similarity transformations. These equations were numerically solved employing fourth order Runge-Kutta algorithm supported by the shooting technique. In the numerical results, the velocity components, shear stress, pressure, temperature and heat flux inside the boundary layer are obtained for various values of nanoparticle volumetric fraction ϕ and different types of nanofluids (silver-water, copper-water, titanium-water and alumina-water). The results shows that the velocity components, temperature and pressure distribution in the boundary layer decrease as increases of nanoparticle volume fraction. To check the behavior and performance of the flow and heat transfer, a comparison of different types of nanofluids is illustrated. It is found that the silver nanoparticles achieve the highest value of temperature due to high thermal conductivity and also they achieve the highest value of pressure due to high density compared to the other nanoparticles. Moreover, the radial velocity and the axial velocity are the highest for titanium oxide-water nanofluid compared to the alumina-water, copper-water and silver water.

1. Introduction

Nanofluid is a recent development in applications of nanotechnology which incorporate small amount of nanosized metallic or non-metallic particles (of range less than 100 nm). These particles are suspended uniformly and stably in a base liquid. The base liquid types are water, oils and ethylene glycol (EG) mixture. The solid nanoparticles distributed in traditional fluids greatly affects their thermal conductivity. The solid particles in nanofluid enhance its characteristics such as a electrical, thermal conductivities and magnetic properties. Nanofluids can be employed in numerous industrial applications such as transformer cooling, electrical cooling, chemical production, advanced nuclear systems, cooling and heating in building, engine cooling and solar water heating. Many researchers were motivated to investigate the behavior of mass and heat characteristics in nanofluids subjected to different flow conditions in various geometries [1, 2] . Two models were used to

* Corresponding author. Tel.: +201224330787.
E-mail address: ahmed.s.rashed@gmail.com, asrashed@zu.edu.eg.

investigate nanofluid behavior, the homogeneous and the non-homogeneous models.

The non-homogeneous model considers the slip motion and related forces, whereas in the homogeneous model, this effect is negligible [3]. In homogeneous model, due to the small size of nanoparticles, the fluid and particles velocity is the same. The properties of the nanofluid were calculated for certain values of Peclet number [4-6]. For a homogeneous analysis, the governing equations are continuity, momentum and energy equations with their physical properties which are related to the volumetric fraction of nanoparticles. Many researchers studied convective transport models of nanofluid in a non-homogeneous model [3, 7, 8]. Buongiorno carried out an comprehensive study of convective transport in nanofluids [9].

In engineering studies, the fluid flow and the corresponding heat mass transfer around cylinders are important since the moving fluid affects the thermal resistance and the cooling of the product. The flow over cylinders is assumed to be two-dimensional when the body radius is large with respect to the boundary layer thickness. In addition, if the cylinder radius is of the same order as the thickness of the boundary layer, the flow is considered axisymmetric [10, 11]. The convective heat transfer for various geometries in nanofluids with different flow conditions has been studied by the Khanafer et al. [1] and Khan and Aziz [12]. Brady and Acrivos [13] studied the steady flow in an incompressible and viscous ambient fluid inside a stretching tube, while Wang [14] examined the same flow outside of a stretching cylinder. Rahman [15] showed that nanofluid flow velocity is lower than base fluid velocity. Also, he found that the presence of nanoparticles improves the rate of heat transfer and decreases the thickness of the hydrodynamic boundary layer. Ferdows [16] concluded that the thermal boundary layer decreases with an increase in the volume fraction of the nanoparticles and increases with an increase in the viscosity. Maskeen [17] indicated that through increasing the impact of magnetic parameter M, the hybrid nanofluids velocity profile decreases but the temperature profile increased. Elgazery [18] found that by using different types of nanofluids, the velocity and temperature profiles were affected, which means that nanofluids are significant in the heating and cooling processes. Also, he found that adding silver oxide achieves the maximum value of the temperature of the nanofluid.

In this study, using group transformation method and similarity transformation, the mathematical model was transformed into a system of ordinary differential equations (ODEs). The system equations of (ODEs) are solved numerically by using shooting technique. Different techniques of similarity transformation were used to investigate either evolutionary equations with different dimensions or fluid dynamics described by Navier-Stokes equations [19-28] . The solution for this set defines the invariants specific form [29].

Nomenclature

Latin symbols

a	Group parameter
G	Group symbol
C_p	Specific heat at constant pressure (J/ Kg K)
K_{bf}	Thermal conductivity of base fluid (W/m K)
K_{nf}	Thermal conductivity of nanofluid (W/m K)
P	Pressure (Pa)
p_w	Wall pressure
Q	Real-valued coefficient
R	Radius of the cylinder
r	Distance along the radial direction (m)
T	Nanofluid temperature (K)
T_w	Temperature at cylinder surface (K)
T_∞	Ambient temperature (K)
u	radial velocity (m/sec)
w	axial velocity (m/sec)
u_w	Wall velocity
w_w	Velocity of the stretching cylinder
z	Distance along the axial direction (m)

Greek symbols

α_{nf}	Effective thermal diffusivity of nanofluid (m^2/sec)
η	Similarity variable
θ	Dimensionless temperature
μ_{bf}	Dynamic viscosity of the base fluid (Pa s)
μ_{nf}	Dynamic viscosity of the nanofluid (Pa s)
υ_{nf}	Kinematic viscosity of nanofluid (m^2/sec)
ρ_{bf}	Density of base fluid (Kg/m^3)
ρ_{nf}	Density of nanofluid (Kg/m^3)
Φ	Solid volume fraction of nanoparticles

Subscript

bf	Base fluid
nf	Nanofluid
sp	Solid Nanoparticle
w	Condition at the surface
∞	Conditions far away from the surface

Superscript

$'$	differentiation with respect to η

2. Mathematical formulation

In the present research, as a function of spatial variables z and r, we found a mathematical analysis for moving a cylinder with radius R through a two – component mixture (homogenous nanofluid) with volumetric fraction of nanoparticles. We considered a homogeneous laminar nanofluid in two dimensions. We further assumed that the nanoparticles in the base fluid are locally in thermal equilibrium. The flow configurations and the geometry of the problem are shown in Figure (1).

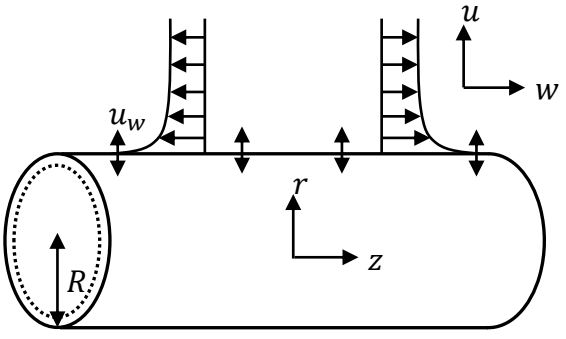

Fig.1.The Physical model and coordinate system

Under the above assumptions, the governing equations can be written in the form:

$$\nabla \cdot V = 0 \qquad (2.1)$$

$$w\,\frac{\partial w}{\partial z} + u\,\frac{\partial w}{\partial r} = \nu_{nf}\left[\frac{\partial^2 w}{\partial r^2} + \frac{1}{r}\,\frac{\partial w}{\partial r}\right] \qquad (2.2)$$

$$w\,\frac{\partial u}{\partial z} + u\,\frac{\partial u}{\partial r} = \frac{-1}{\rho_{nf}}\frac{\partial p}{\partial r} + \nu_{nf}\left[\frac{\partial^2 u}{\partial r^2} + \frac{1}{r}\,\frac{\partial u}{\partial r} - \frac{u}{r^2}\right] \qquad (2.3)$$

$$V \cdot \nabla T = \alpha_{nf}\left[\frac{\partial^2 T}{\partial r^2} + \frac{1}{r}\,\frac{\partial T}{\partial r}\right] \qquad (2.4)$$

The appropriate boundary conditions for this model are:

(i) At the surface of the cylinder $(r = R)$

$$u(z,R) = u_w(z), w(z,R) = w_w(z),\quad p(z,R) = p_w(z), T(z,R) = T_w \qquad (2.5)$$

(ii) Matching with the quiescent free stream $(r \to \infty)$

$$w(z,\infty) = 0, T(z,\infty) = T_\infty \qquad (2.6)$$

Where T_w is the surface temperature of the cylinder and T_∞ is the ambient temperature.

Thermophysical properties of nanofluid:

The physical quantities $\rho_{bf}, (C_p)_{bf}, \mu_{bf}$, and k_{bf} are the density, specific heat, dynamic viscosity, and thermal conductivity of the base fluid while $\rho_{sp}, (C_p)_{sp}, \mu_{sp}$, and k_{sp}, respectively are the solid nanoparticles properties.

The physical quantities are presented as follows [30]:

$$\rho_{nf} = \rho_{bf}(1-\phi) + \rho_{sp}\phi,$$
$$(\rho C_p)_{nf} = (\rho C_p)_{bf}(1-\phi) + (\rho C_p)_{sp}\phi,$$
$$k_{nf} = \left(\frac{k_{sp}+2k_{bf}-2\phi(k_{bf}-k_{sp})}{k_{sp}+2k_{bf}+\phi(k_{bf}-k_{sp})}\right)k_{bf},$$
$$\mu_{nf} = \frac{\mu_{bf}}{(1-\phi)^{2.5}},\quad \nu_{nf} = \frac{\mu_{nf}}{\rho_{nf}},\quad \alpha_{nf} = \frac{k_{nf}}{(\rho C_p)_{nf}} \qquad (2.7)$$

Where ϕ is the volume fraction of nanoparticle, ν_{nf} is the kinematic viscosity and α_{nf} is the effective thermal diffusivity of nanofluid. Thermophysical properties are illustrated in Table 1. The dynamic viscosity (μ_{bf}) of pure water is equal to 1.07 mPa s and the dynamic viscosity of Kerosene is equal to 1.92 mPa s.

Table 1. Physical properties of the base fluid and nanoparticles[31, 32]

Physical properties		ρ (kg/m^3)	C_p (J/kgK)	k (w/mK)
Base fluids	Water (H_2O)	997.1	4179	0.613
	Kerosene	780	2090	0.149
Nanoparticles	Silver (Ag)	10500	235	429
	Copper (Cu)	8933	385	400
	Alumina (AL_2O_3)	3970	765	40
	Titanium oxide (TiO_2)	4250	686.2	8.9538

The following transformations are used to normalize the boundary conditions:

$$u(z,r) = u_w(z)U(z,r), w(z,r) = w_w(z)W(z,r)$$
$$p(z,r) = p_w(z)P(z,r), \theta = \frac{T-T_\infty}{T_w-T_\infty} \qquad (2.8)$$

By using (2.8), the mathematical model and the corresponding boundary conditions, (2.1)-(2.6), are transformed into:

$$W\,\frac{\partial w_w}{\partial z} + w_w\,\frac{dw}{dz} + u_w\,\frac{\partial u}{\partial r} + \frac{Uu_w}{r} = 0 \qquad (2.9)$$

$$Ww_w\left(W\frac{\partial w_w}{\partial z}+w_w\frac{\partial W}{\partial z}\right)+Uu_w\left(w_w\frac{\partial W}{\partial r}\right)=\nu_{nf}\left[w_w\frac{\partial^2 W}{\partial r^2}+\frac{1}{r}\,w_w\frac{\partial w}{\partial r}\right] \quad (2.10)$$

$$Ww_w\left(U\frac{\partial u_w}{\partial z}+u_w\frac{\partial U}{\partial z}\right)+Uu_w\left(u_w\frac{\partial U}{\partial r}\right)=-\frac{p_w}{\rho_{nf}}\frac{\partial P}{\partial r}+\nu_{nf}\left[u_w\frac{\partial^2 U}{\partial r^2}+\frac{1}{r}\,u_w\frac{\partial U}{\partial r}-\frac{u_w U}{r^2}\right] \quad (2.11)$$

$$w_w W(\Delta T)\frac{\partial\theta}{\partial z}+u_w U(\Delta T)\frac{\partial\theta}{\partial r}=\alpha_{nf}\left[(\Delta T)\frac{\partial^2\theta}{\partial r^2}+\frac{1}{r}(\Delta T)\,\frac{\partial\theta}{\partial r}\right] \quad (2.12)$$

Subjected to:

$$U(z,\,r_0)=1, W(z,\,r_0)=1,\\ P(z,r_0)=1,\theta(z,\,r_0)=1 \quad (2.13)$$

$$W(z,\infty)=0,\theta(z,\infty)=1 \quad (2.14)$$

3. Group formulation of the problem

The governing equations of (2.9) to (2.12) were transformed into a system of ODEs with respect to the similarity variable. This technique is based on a transformation class, that is, one parameter group *G*:

$$G:\ \bar{S}=Q^s(a)S+T^S(a) \quad (3.1)$$

Where S and $\bar{S}$ represents the system variables before and after the transformation as well as Q^s And $T^s$are real valued and at least differentiable in the real argument(a). The partial derivatives of the dependent variables can now be calculated as seen with respect to the independent variables:

$$\left.\begin{array}{l}\bar{S}_{\bar{i}}=\left(\frac{Q^S}{Q^i}\right)S_i\\ \bar{S}_{\bar{i}\,\bar{j}}=\left(\frac{Q^S}{Q^iQ^j}\right)S_{ij}\end{array}\right\}\ i,j=z,r \quad (3.2)$$

Where S represents the dependent variables ($W, w_w\ U, u_w, P, p_w and\ \theta$)
A transformation of equations (2.9)-(2.12) following the definitions (3.1) and (3.2) yields to:

$$\bar{W}\,\frac{\partial\bar{w}_w}{\partial\bar{z}}+\bar{w}_w\,\frac{\partial\bar{w}}{d\bar{z}}+\bar{u}_w\,\frac{\partial\bar{u}}{\partial\bar{r}}+\frac{\bar{U}\bar{u}_w}{\bar{r}}=H_1(a)\left[W\,\frac{\partial w_w}{\partial z}+w_w\,\frac{dw}{dz}+u_w\,\frac{\partial u}{\partial r}+\frac{Uu_w}{r}\right] \quad (3.3)$$

$$\bar{w}_w\bar{W}\left(\bar{w}_w\frac{\partial\bar{W}}{\partial\bar{z}}+\bar{W}\frac{\partial\bar{w}_w}{\partial\bar{z}}\right)+\bar{u}_w\bar{U}\left(\bar{w}_w\frac{\partial\bar{W}}{\partial\bar{r}}\right)-\nu_{nf}\left[\bar{w}_w\frac{\partial^2\bar{W}}{\partial\bar{r}^2}+\frac{1}{\bar{r}}\,\bar{w}_w\frac{\partial\bar{w}}{\partial\bar{r}}\right]=H_2(a)\left[\begin{array}{c}w_w\bar{W}\left(w_w\frac{\partial W}{\partial z}+W\frac{\partial w_w}{\partial z}\right)+u_wU\left(w_w\frac{\partial W}{\partial r}\right)\\ -\nu_{nf}\left[w_w\frac{\partial^2 W}{\partial r^2}+\frac{1}{r}\,w_w\frac{\partial w}{\partial r}\right]\end{array}\right] \quad (3.4)$$

$$\bar{w}_w\bar{W}\left(\bar{u}_w\frac{\partial\bar{u}}{\partial\bar{z}}+\bar{U}\frac{\partial\bar{u}_w}{\partial\bar{z}}\right)+\bar{u}_w\bar{U}\left(\bar{u}_w\frac{\partial\bar{U}}{\partial\bar{r}}\right)+\frac{\bar{p}_w}{\rho_{nf}}\frac{\partial\bar{P}}{\partial\bar{r}}-\nu_{nf}\left[\bar{u}_w\frac{\partial^2\bar{U}}{\partial\bar{r}^2}+\frac{1}{\bar{r}}\,\bar{u}_w\frac{\partial\bar{U}}{\partial\bar{r}}-\frac{\bar{u}_w\bar{U}}{\bar{r}^2}\right]=H_3(a)\left[\begin{array}{l}w_wW\left[u_w\frac{\partial U}{\partial z}+U\frac{\partial u_w}{\partial z}\right]+u_wU\left[u_w\frac{\partial U}{\partial r}\right]+\\ \frac{p_w}{\rho_{nf}}\frac{\partial P}{\partial r}-\nu_{nf}\left[\begin{array}{c}u_w\frac{\partial^2 U}{\partial r^2}-\frac{u_wU}{r^2}\\ +\frac{1}{r}\,u_w\frac{\partial U}{\partial r}\end{array}\right]\end{array}\right] \quad (3.5)$$

$$\bar{w}_w\bar{W}(\Delta T)\frac{\partial\bar{\theta}}{\partial\bar{z}}+\bar{u}_w\bar{U}(\Delta T)\frac{\partial\bar{\theta}}{\partial\bar{r}}-\alpha_{nf}\left[(\Delta T)\frac{\partial^2\bar{\theta}}{\partial\bar{r}^2}+\frac{1}{\bar{r}}(\Delta T)\,\frac{\partial\bar{\theta}}{\partial\bar{r}}\right]=H_4(a)\left[w_wW(\Delta T)\frac{\partial\theta}{\partial z}+u_wU(\Delta T)\frac{\partial\theta}{\partial r}-\alpha_{nf}\left[(\Delta T)\frac{\partial^2\theta}{\partial r^2}+\frac{1}{r}(\Delta T)\,\frac{\partial\theta}{\partial r}\right]\right] \quad (3.6)$$

The invariant transformation of (3.3) - (3.6) and invariance of boundary conditions (2.13) are used to obtain the following results:

$$T^W=T^{w_w}=T^U=T^{u_w}=T^P=T^{p_w}=T^\theta=T^r=0 \quad (3.7)$$

$$\frac{Q^{w_w}Q^w}{Q^z}=\frac{Q^{u_w}Q^U}{Q^r}=H_1(a) \quad (3.8)$$

$$\frac{\left(Q^{w_w}Q^W\right)^2}{Q^z}=\frac{Q^{w_w}Q^w}{(Q^r)^2}=\frac{Q^{w_w}Q^wQ^{U_w}Q^U}{Q^r}=H_2(a) \quad (3.9)$$

$$\frac{\left(Q^{u_w}Q^U\right)^2}{Q^r}=\frac{Q^{u_w}Q^U}{(Q^r)^2}=\frac{Q^{w_w}Q^wQ^{U_w}Q^U}{Q^z}=\frac{Q^{p_w}Q^P}{Q^r}=H_3(a) \quad (3.10)$$

$$\frac{Q^{w_w}Q^WQ^\theta}{Q^z}=\frac{Q^{u_w}Q^UQ^\theta}{Q^r}=\frac{Q^\theta}{(Q^r)^2}=H_4(a) \quad (3.11)$$

The combination of equations (3.7) - (3.11) will lead to:

$$Q^z=(Q^r)^4,\ Q^\theta=(Q^r)^2 \quad (3.12)$$

$$Q^U=\frac{1}{Q^rQ^{u_w}},Q^W=\frac{(Q^r)^2}{Q^{w_w}},Q^P=\frac{1}{(Q^r)^2\,Q^{p_w}} \quad (3.13)$$

The group G is of the form:

$$G\begin{cases} G_1 \begin{cases} \bar{z} = (Q^r)^4 z + T^z \\ \bar{r} = Q^r r \end{cases} \\ G_2 \begin{cases} \bar{U} = \frac{1}{Q^r Q^{u_w}} U \\ \bar{u}_w = Q^{u_w} u_w \\ \bar{W} = \frac{(Q^r)^2}{Q^{w_w}} W \\ \bar{w}_w = Q^{w_w} w_w \\ \bar{P} = \frac{1}{(Q^r)^2\, Q^{p_w}} P \\ \bar{p}_w = Q^{p_w} p_w \\ \bar{\theta} = (Q^r)^2 \theta \end{cases} \end{cases} \quad (3.14)$$

Where G_1 is the independent variables and G_2 is the dependent variables.

3.1. Group transformation of the system

According to the fundamental Morgan theorem [33], the system of ODEs was obtained from the governing equations.

$$\sum_{i=1}^{9} (\alpha_i s_i + \beta_i) \frac{\partial \bar{s}_i}{\partial s_i} = 0 \quad (3.15)$$

Where the coefficients α_i and β_i are defined as:

$$\alpha_i = \frac{\partial Q^{si}(a)}{\partial a}\ ,\ \beta_i = \frac{\partial T^{si}(a)}{\partial a} \quad (3.16)$$

3.2. Transformation of the independent variables

The similarity variable $\eta(z,r)$ was obtained by applying the equation (3.15):

$$(\alpha_1 z + \beta_1) \frac{\partial \eta}{\partial z} + \alpha_2 r \frac{\partial \eta}{\partial r} = 0 \quad (3.17)$$

The general solution of this equation is shown as:

$$\eta(z,r) = r\, \pi(z) \quad (3.18)$$

Where, the function $\pi(z)$ will be defined later.

3.3 Transformation of the dependent variables

The invariant transformations of the dependent variables $\bar{p}_w, \bar{P}, \bar{w}_w, \bar{W}, \bar{u}_w, \bar{U}$ and $\bar{\theta}$ inside the boundary layer are obtained from the group structure (3.14) and the Morgan theorem described in (3.15):

$$\bar{p}_w(\bar{z}) = p_w(z) \quad (3.19)$$

$$\bar{P}(\bar{z},\bar{r}) = \psi(z) g(\eta) \quad (3.20)$$

$$\bar{w}_w(\bar{z},\bar{r}) = w_w(z) \quad (3.21)$$

$$\bar{w}(\bar{z},\bar{r}) = \Gamma(z) E(\eta) \quad (3.22)$$

$$\bar{u}_w(\bar{z}) = u_w(z) \quad (3.23)$$

$$\bar{U}(\bar{z},\bar{r}) = \omega(z) F(\eta) \quad (3.24)$$

$$\bar{\theta}(\bar{z},\bar{r}) = \varepsilon(z) q(\eta) \quad (3.25)$$

3.4. Reduction of the problem to a system of ordinary differential equations

By using similarity variables, the equations from (2.9) – (2.12) can now be written as:

Hence, Eq. (2.9) takes the form:

$$\frac{dF}{d\eta} + (A_1 + A_2) E + A_3\, \eta \frac{dE}{d\eta} + \frac{F}{\eta} = 0 \quad (3.26)$$

Where:

$$A_1 = \frac{w_w\, (d\Gamma/dz)}{\omega u_w \pi}, A_2 = \frac{\Gamma\, (dw_w/dz)}{\omega u_w \pi}, A_3 = \frac{\Gamma\, w_w\ (d\pi/dz)}{\omega u_w \pi^2} \quad (3.27)$$

Similarly, equation (2.10) is reduced to:

$$\frac{d^2E}{d\eta^2} - (A_4 + A_5) E^2 - A_6 \eta E \frac{dE}{d\eta} - A_7 F \frac{dE}{d\eta} + \frac{1}{\eta} \frac{dE}{d\eta} = 0 \quad (3.28)$$

Where:

$$A_4 = \frac{\Gamma\, (dw_w/dz)}{\nu \pi^2}, A_5 = \frac{w_w\, (d\Gamma/dz)}{\nu \pi^2},$$
$$A_6 = \frac{\Gamma\, w_w\, (d\pi/dz)}{\nu \pi^3}, A_7 = \frac{\omega\, u_w}{\nu \pi} \quad (3.29)$$

Similarly, equation (2.11) is reduced to:

$$\frac{d^2F}{d\eta^2} - A_6 \eta E \frac{dF}{d\eta} - A_7 F \frac{dF}{d\eta} - (A_8 + A_9) EF - A_{10} \frac{1}{\rho_{nf}} \frac{dg}{d\eta} + \frac{1}{\eta} \frac{dF}{d\eta} + \frac{F}{\eta^2} = 0 \quad (3.30)$$

Where:

$$A_8 = \frac{\Gamma\, w_w\, (du_w/dz)}{\nu u_w \pi^2}, A_9 = \frac{\Gamma\, w_w\, (d\omega/dz)}{\nu\, \omega \pi^2},$$
$$A_{10} = \frac{P\, \psi}{\nu\, \omega\, u_w \pi} \quad (3.31)$$

If the coefficients stated by (3.27), (3.29) and (3.31) are constants or functions of η alone, the equations

(3.26), (3.28) and (3.30) will be reduced to system of ODEs. Thus:

$$u_w(z) = w_w(z) = (mvz + b), \varepsilon(z) = (mvz + b),$$
$$\pi(z) = \psi(z) = (mvz + b)^{\frac{1}{m}}, \Gamma(z) = (mvz + b)^{\frac{2}{m}},$$
$$\omega(z) = v(mvz + b)^{\frac{1}{m}-1}, p_w(z) = v\,(mvz + b)^{\frac{1}{m}},$$
$$\eta(z,r) = r(mvz + b)^{\frac{1}{m}} \qquad (3.32)$$

And $A_1 = A_5 = 2, A_2 = A_4 = A_8 = m,$
$A_3 = A_6 = A_7 = 1, A_9 = (1 - m), A_{10} = \frac{1}{v_{nf}}$ *(3.33)*

Where, m is a constant and $m \neq 0$ *or* 1.
By substituting for these constants, Hence, Eq. (2.12) takes the form:

$$q'' = \frac{v_{nf}}{\alpha_{nf}}(\eta E q' + mEq + Fq') - \frac{q'}{\eta} \qquad (3.34)$$

The boundary conditions under the similarity variable are:

$$F(1) = 1, E(1) = 1, g(1) = 1, q(1) = 1,$$
$$F(\infty) = 0.2, E(\infty) = 0, q(\infty) = 0 \qquad (3.35)$$

4. Numerical results and discussion

In order to analyze the results, the ordinary differential equations (3. 26) - (3.34) subject to the boundary conditions (3.35) were numerically solved using fourth order Runge-Kutta algorithm supported by the shooting technique. The parameters of the analysis are the effect of volumetric fraction of the nanoparticles, ϕ, and the different types of nanoparticles. By using water as a base fluid, the different types of nanoparticles, alumina (Al_2O_3) silver (Ag), titanium oxide (TiO_2) and copper (Cu).

4.1 Effect of nanoparticle volume fraction, ϕ

In these calculations, parameter ϕ represents the nanoparticle volume fraction of nanofluid with range $2\% \leq \phi \leq 10\%$. The results showed that increasing the volume fraction (ϕ) of nanoparticles decreases the radial velocity (F) and the peak value of the axial velocity(E) as shown in Figures 2 and 3, respectively.
Because increasing the volume fraction (ϕ) of nanoparticles made some obstacles towards the fluid flow . Following this the related shear stress (F') and (E') decreases near the cylinder surface and increases away from the cylinder surface when ϕ increases as shown in Figures 4 and 5, respectively. Figure 6 shows that the increment in the values of volume fraction ϕ decreases the temperature distribution. As a result, the heat flux increases when ϕ increases as illustrated in Figure 7. Moreover, the pressure distribution in the boundary layer decreases when ϕ increases as shown in Figure 8.

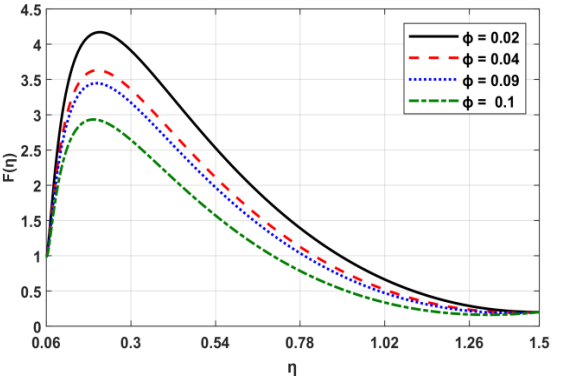

Fig.2 Effect of nanoparticle volume fraction (ϕ) on radial velocity (F) inside the boundary layer of (Al2O3-water)

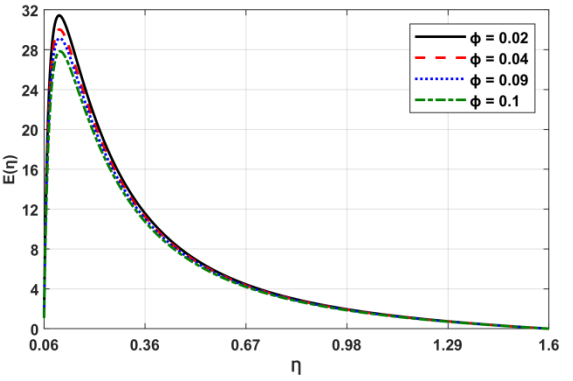

Fig.3 Effect of nanoparticle volume fraction (ϕ) on axial velocity (E) inside boundary layer of (Al2O3-water)

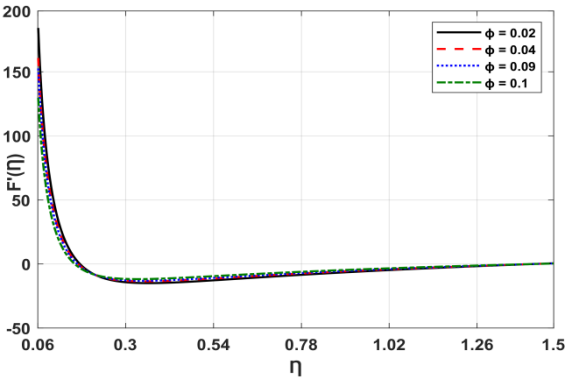

Fig.4 Effect of nanoparticle volume fraction (ϕ) on shear stress (F′) inside the boundary layer of (Al2O3-water)

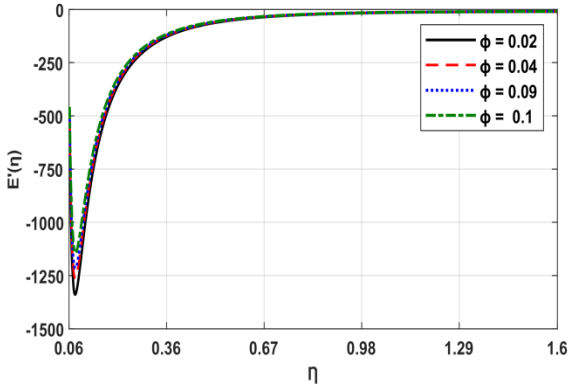

Fig.5 Effect of nanoparticle volume fraction (ϕ) on shear stress (E′) inside the boundary layer of (Al2O3-water)

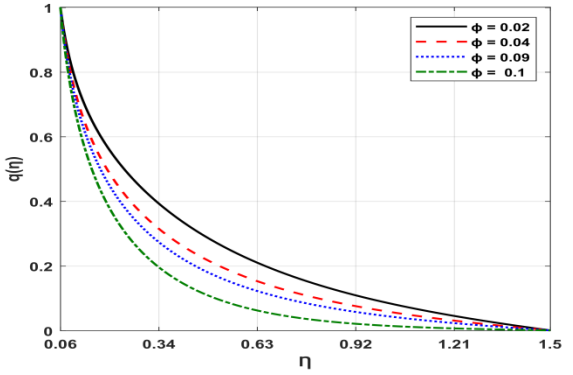

Fig.6 Effect of nanoparticle volume fraction (ϕ) on temperature distribution (q) inside the boundary layer of (Al2O3-water)

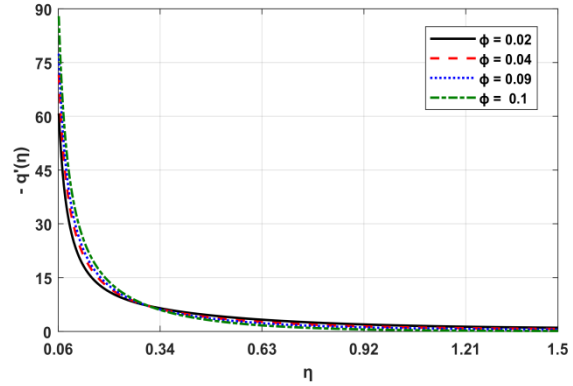

Fig.7 Effect of nanoparticle volume fraction (ϕ) on heat flux (q′) inside the boundary layer of (Al2O3-water)

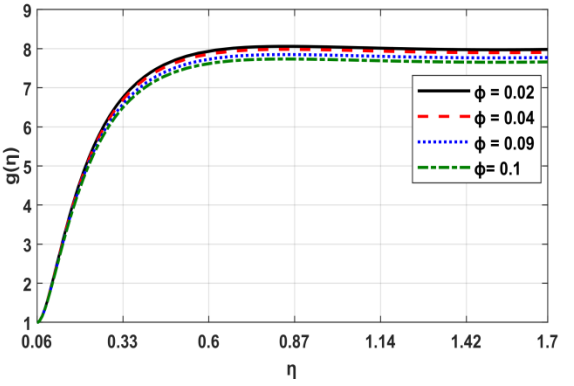

Fig.8 Effect of nanoparticle volume fraction (ϕ) on pressure (g) inside the boundary layer of (Al2O3-water)

4.2 Effect of different types of nanoparticles, Ag, Cu, TiO_2 and Al_2O_3

The thermophysical properties of nanoparticles are described in Table 1. The physical properties of the nanofluids are plotted at fixed value of volume fraction $\phi = 0.097$.

In Figures 9, 10 and 11, we see that the radial velocity (F), the peak value of the axial velocity (E) and the related shear stress (F') are the highest for the titanium-water (TiO_2-H_2O) nanofluid compared to the other nanofluids (Al_2O_3-H_2O, Cu-H_2O and Ag-H_2O). On contrary, the highest value of the shear stress (E') is obtained for the silver-water nanofluid, but the lowest value is obtained for the titanium oxide-water nanofluid as shown in Figure 12. Additionally, Figure 13 indicates that the maximum temperature value is obtained by adding silver oxide to the fluid, while the minimum temperature value is obtained by using titanium oxide as a nanoparticle. As observed in Figure 14, the results for the heat flux are reversed. As shown in Figure 15, the pressure for the silver-water nanofluid is the highest pressure compared to the other nanofluids. This is because silver has the highest value of density compared to the other nanofluids, as seen in Table 1.

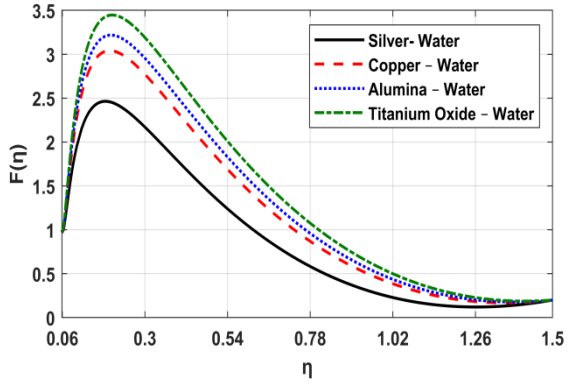

Fig.9 Effect of different types of nanofluids on radial velocity (F) inside the boundary layer

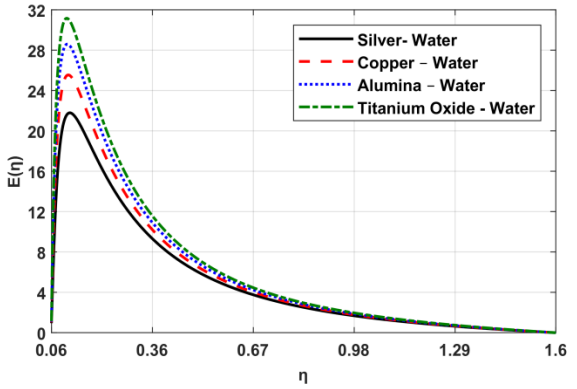

Fig.10 Effect of different types of nanofluids on axial velocity (E) inside the boundary

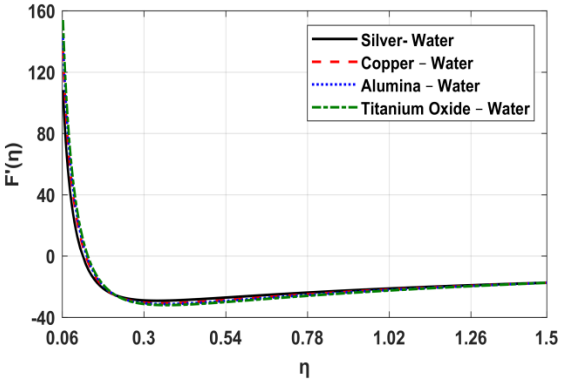

Fig.11 Effect of different types of nanofluids on shear stress (F′) inside the boundary layer

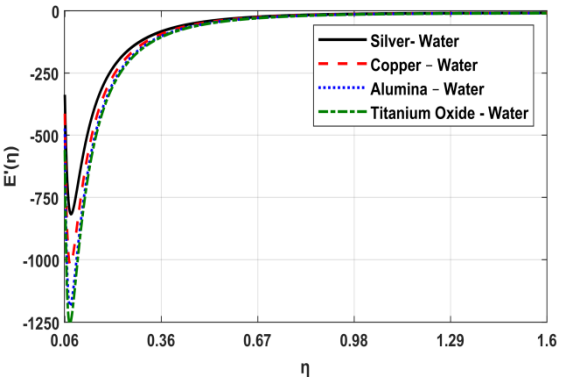

Fig.12 Effect of different types of nanofluids on shear stress (E′) inside the boundary layer

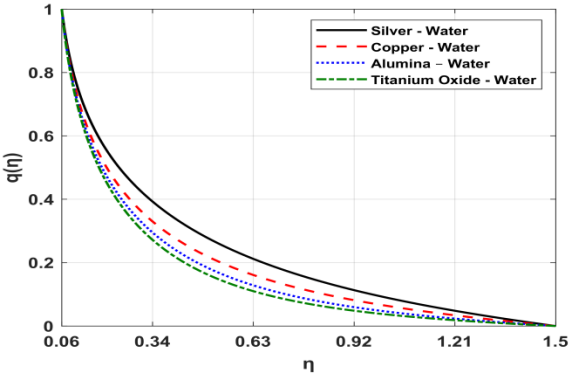

Fig.13 Effect of different types of nanofluids on temperature distribution (q)inside the boundary layer

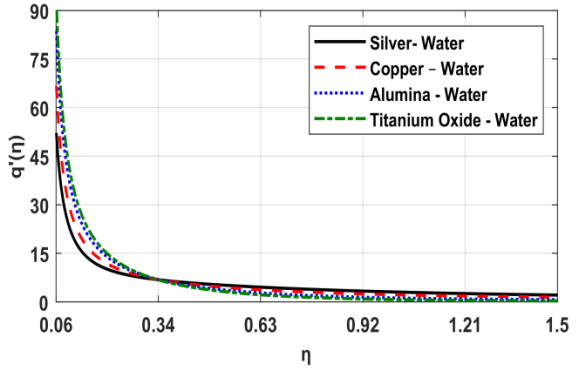

Fig.14 Effect of different types of nanofluids on heat flux (q′) inside the boundary

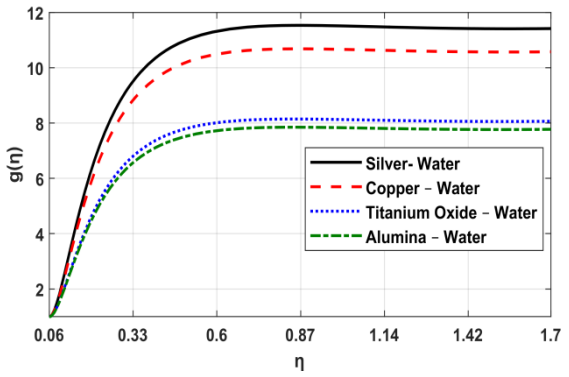

Fig.15 Effect of different types of nanofluids on pressure (g) inside the boundary layer

Several researchers investigated the flow and heat transfer for various values of volume fraction of nanoparticles. Additionally, to check its heat transfer performance they studied different types of nanofluids with various geometries.

In case of studying of the volume fraction, it was observed that increasing of volume fraction (ϕ) leads to decrease the temperature distribution [34-36]. Additionally, increasing volume fraction decreases the velocity [37, 38]. The same conclusion was achieved in the current work for the effect of the volume fraction in Figures 2, 3 and 6.

In case of studying of different types of nanofluids, it was observed that the silver has the highest value of temperature compared to the copper-water , alumina-water and titanium- water [18, 39]. On the other hand, the highest value of the velocity was obtained for the titanium oxide-water nanofluid [16, 18] . The same sequence of nanofluids was obtained in this work in Figures 9, 10 and 13.

Relating to the mentioned studies, we found that there is a very good agreement between the obtained results and the previous results.

For validation of the numerical method used in this study, the present results are compared to the results reported by researchers [16, 32, 34] as shown in Figs. 16-19.

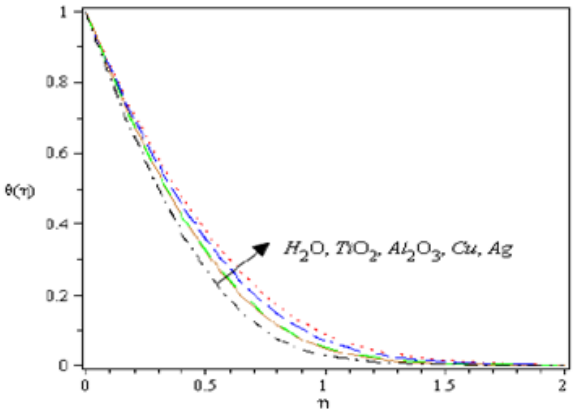

(a) Ferdows et al. work [16]

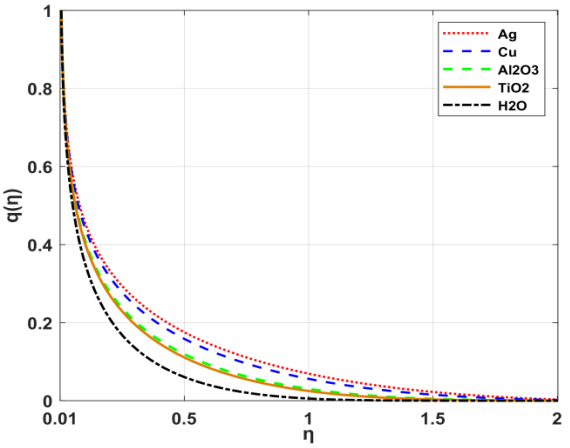

(b) Present work

Fig.16 Effect of different types of nanoparticles and water on temperature distribution (q) inside the boundary layer when $\phi = 0.2$

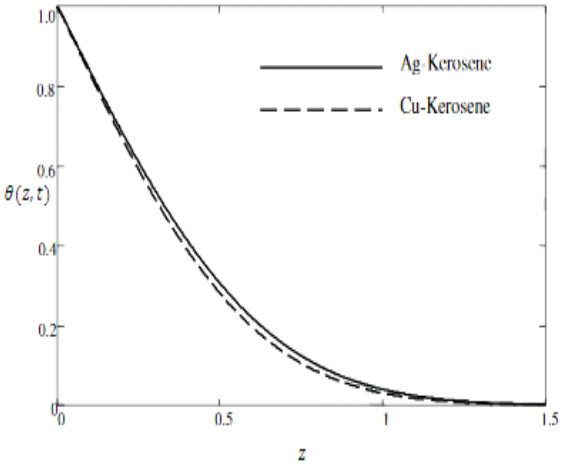

(a) Mohd et al. work [32]

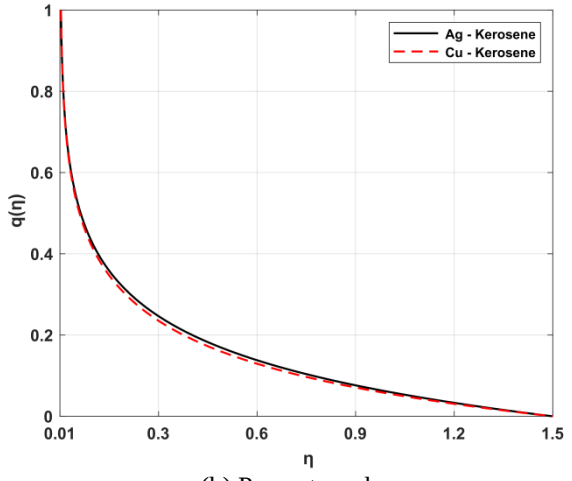

(b) Present work

Fig.17 Effect of different types of nanoparticles with Kerosene as a base fluid on temperature distribution (q) inside the boundary layer when $\phi = 0.2$

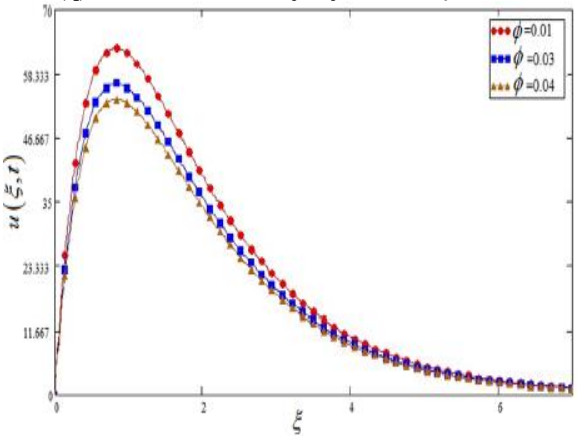

(a) Khan et al. work [37]

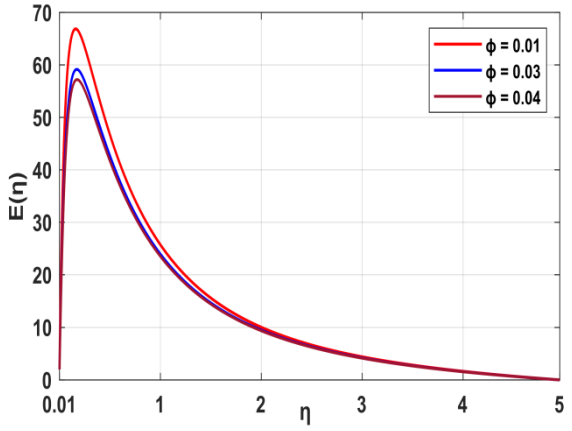

(b) Present work

Fig.18 Effect of nanoparticle volume fraction on the velocity of (TiO2- Sodium alginate)

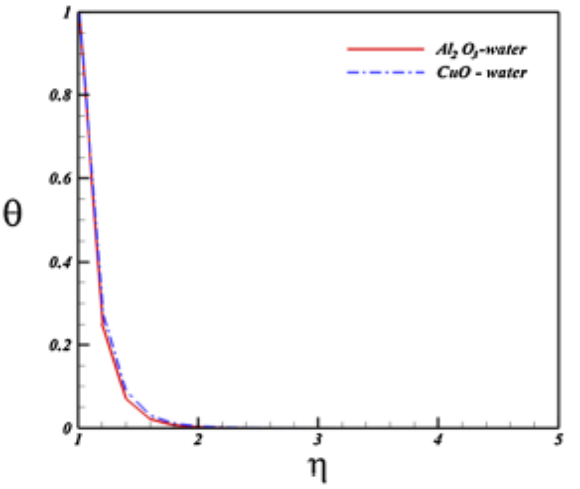

(a) Sheikholeslami work [34]

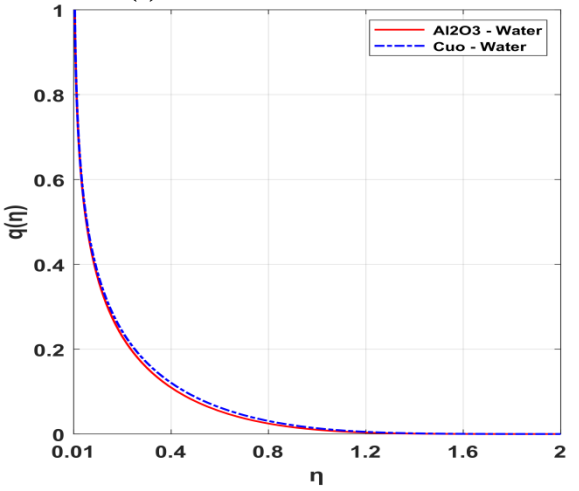

(b) Present work

Fig.19Effect of different types of nanofluids on temperature distribution (q) inside the boundary layer when $\phi = 0.04$

Figures 16-19 indicate that there is a good agreement with these approaches and thus the accuracy of the present used method is verified.

5. Conclusion

The flow and heat transfer in water based nanofluids surrounding a cylindrical solid pipe were studied via group method in this paper. The mathematical model of the problem was transformed into nonlinear ODEs using similarity transformations, which are subsequently solved using MATLAB. The results showed the components of nanofluid velocity, the shear stress components, temperature distribution, the heat flux and pressure distribution. The present study concluded as follows: owing to natural

convection, presence of nanoparticles decreased the value of velocity components, temperature and pressure distribution inside the boundary layer. On the other hand, the shear stress components far away the cylinder surface and heat flux increased as volume fraction ϕ increased.

Nanoparticles with higher friction coefficient on the surface of the cylinder have low speed. The thickness of thermal boundary layer is related to the increase in thermal conductivity of various types of nanofluids, while the effect of pressure is related to the increase in the density. The volume fraction and different types of nanoparticles have more effect on the radial velocity and axial velocity.

Nanofluid type is a key factor in enhancing the heat transfer. Titanium oxide–water and silver–water nanofluids have the highest and the lowest velocity components, respectively, compared to other nanofluids. Using silver nanoparticles would get the highest value for the temperature and pressure compared to the other nanoparticles.

References

[1] K. Khanafer, K. Vafai, and M. Lightstone, "Buoyancy-driven heat transfer enhancement in a two-dimensional enclosure utilizing nanofluids," International journal of heat and mass transfer., vol. 46, pp. 3639-3653, 2003.

[2] E. Abu-Nada, Z. Masoud, and A. Hijazi, "Natural convection heat transfer enhancement in horizontal concentric annuli using nanofluids," International Communications in Heat and Mass Transfer International Communications in Heat and Mass Transfer, vol. 35, pp. 657-665, 2008.

[3] M. Sheikholeslami and D. D. Ganji, "Numerical investigation for two phase modeling of nanofluid in a rotating system with permeable sheet," Journal of Molecular Liquids, vol. 194, pp. 13-19, 2014.

[4] M. Sheikholeslami, D. D. Ganji, and H. R. Ashorynejad, "Investigation of squeezing unsteady nanofluid flow using ADM," Powder Technology, vol. 239, pp. 259-265, 2013.

[5] M. Sheikholeslami and D. D. Ganji, "Heat transfer of Cu-water nanofluid flow between parallel plates," Powder Technology Powder Technology, vol. 235, pp. 873-879, 2013.

[6] Y. Ding and D. Wen, "Particle migration in a flow of nanoparticle suspensions," Powder Technology Powder Technology, vol. 149, pp. 84-92, 2005.

[7] M. Sheikholeslami and H. B. Rokni, "Nanofluid two phase model analysis in existence of induced magnetic field," International journal of heat and mass transfer., vol. 107, pp. 288-299, 2017.

[8] M. Sheikholeslami and D. D. Ganji, "Nanofluid hydrothermal behavior in existence of Lorentz forces considering Joule heating effect," J Mol Liq Journal of Molecular Liquids, vol. 224, pp. 526-537, 2016.

[9] J. Buongiorno, "Convective Transport in Nanofluids," TRANSACTIONS- AMERICAN SOCIETY OF MECHANICAL ENGINEERS JOURNAL OF HEAT TRANSFER, vol. 128, pp. 240-250, 2006.

[10] P. Datta, D. Anilkumar, S. Roy, and N. C. Mahanti, "Effect of non-uniform slot injection (suction) on a forced flow over a slender cylinder," International journal of heat and mass transfer., vol. 49, pp. 2366-2371, 2006.

[11] M. Kumari and G. Nath, "Mixed convection boundary layer flow over a thin vertical cylinder with localized injection/suction and cooling/heating," International Journal of Heat and Mass Transfer, vol. 47, pp. 969-976, 2004.

[12] W. A. Khan and A. Aziz, "Natural convection flow of a nanofluid over a vertical plate with uniform surface heat flux," International Journal of Thermal Sciences International Journal of Thermal Sciences, vol. 50, pp. 1207-1214, 2011.

[13] J. F. Brady and A. Acrivos, "Steady flow in a channel or tube with an accelerating surface velocity. An exact solution to the NavierStokes equations with reverse flow," J. Fluid Mech. Journal of Fluid Mechanics, vol. 112, p. 127, 1981.

[14] C. Y. Wang, "Fluid flow due to a stretching cylinder," Phys. Fluids Physics of Fluids, vol. 31, p. 466, 1988.

[15] M. Rahmana and A. Aziz, "HEAT TRANSFER IN WATER BASED NANOFLUIDS (TiO2-H2O, Al2O3-H2O and Cu-H2O) OVER A STRETCHING CYLINDER," IJHT International Journal of Heat and Technology, vol. 30, pp. 31-42, 2012.

[16] M. Ferdows, S. Islam, and R. A. Quadir, "Similarity solutions of Marangoni heat transfer flow of water based nanofluid containing nanoparticles with variable viscosity and thermal conductivity," Int. Rev. Mech. Eng. International Review of Mechanical Engineering, vol. 7, pp. 692-697, 2013.

[17] M. M. Maskeen, A. Zeeshan, O. U. Mehmood, and M. Hassan, "Heat transfer enhancement in hydromagnetic aluminacopper/water hybrid nanofluid flow over a stretching cylinder," J Therm Anal Calorim Journal of Thermal Analysis and Calorimetry, vol. 138, pp. 1127-1136, 2019.

[18] N. S. Elgazery, "Nanofluids flow over a permeable unsteady stretching surface with non-uniform heat source/sink in the presence of inclined magnetic field," J Egypt Math Soc Journal of the Egyptian Mathematical Society, vol. 27, pp. 1-26, 2019.

[19] M. Kassem, "Group solution for unsteady free-convection flow from a vertical moving plate subjected to constant heat flux," Journal of Computational and Applied Mathematics, vol. 187, pp. 72-86, 2006.

[20] A. S. Rashed and M. M. Kassem, "Group analysis for natural convection from a vertical plate," Journal of Computational and Applied Mathematics, vol. 222, pp. 392-403, 2008/12/15/ 2008.

[21] M. M. Kassem and A. S. Rashed, "Group solution of a time dependent chemical convective process," Applied Mathematics and Computation, vol. 215, pp. 1671-1684, 2009.

[22] A. S. Rashed and M. M. Kassem, "Hidden symmetries and exact solutions of integro-differential Jaulent–Miodek evolution equation," Applied Mathematics and Computation, vol. 247, pp. 1141-1155, 2014/11/15/ 2014.

[23] S. M. Mabrouk and A. S. Rashed, "Analysis of (3 + 1)-dimensional Boiti–Leon–Manna–Pempinelli equation via Lax pair investigation and group transformation method," Computers & Mathematics with Applications, vol. 74, pp. 2546-2556, 2017/11/15/ 2017.

[24] A. S. Rashed, "Analysis of (3+1)-dimensional unsteady gas flow using optimal system of Lie symmetries," Mathematics and Computers in Simulation, vol. 156, pp. 327-346, 2019/02/01/ 2019.

[25] M. M. Kassem and A. S. Rashed, "N-solitons and cuspon waves solutions of $(2+1)$-dimensional Broer–Kaup–Kupershmidt equations via hidden symmetries of Lie optimal system," Chinese Journal of Physics, vol. 57, pp. 90-104, 2019/02/01/ 2019.

[26] S. M. Mabrouk and A. S. Rashed, "N-Solitons, kink and periodic wave solutions for (3 + 1)-dimensional Hirota bilinear equation using three distinct techniques," Chinese Journal of Physics, vol. 60, pp. 48-60, 2019/08/01/ 2019.
[27] R. Saleh and A. S. Rashed, "New exact solutions of (3 + 1)-dimensional generalized Kadomtsev-Petviashvili equation using a combination of lie symmetry and singular manifold methods," Mathematical Methods in the Applied Sciences, vol. 43, pp. 2045-2055, 2020/03/15 2020.
[28] A. S. Rashed, S. M. Mabrouk, and A.-M. Wazwaz, "Forward scattering for non-linear wave propagation in (3 + 1)-dimensional Jimbo-Miwa equation using singular manifold and group transformation methods," Waves in Random and Complex Media, pp. 1-13, 2020.
[29] M. J. Moran, R. A. Gaggioli, and W. B. Scholten, A new systematic formalism for similarity analysis, with applications to boundary layer flows. Madison, Wis: Mathematics Research Center, United States Army, Univ. of Wisconsin, 1968.
[30] S. M. Aminossadati and B. Ghasemi, "Natural convection cooling of a localised heat source at the bottom of a nanofluid-filled enclosure," European Journal of Mechanics - B/Fluids, vol. 28, pp. 630-640, 2009/09/01/ 2009.
[31] E. Abu-Nada and H. F. Oztop, "Effects of inclination angle on natural convection in enclosures filled with Cu–water nanofluid," International Journal of Heat and Fluid Flow, vol. 30, pp. 669-678, 2009/08/01/ 2009.
[32] N. A. Mohd Zin, I. Khan, S. Shafie, and A. S. Alshomrani, "Analysis of heat transfer for unsteady MHD free convection flow of rotating Jeffrey nanofluid saturated in a porous medium," Results in Physics, vol. 7, pp. 288-309, 2017/01/01/ 2017.
[33] A. J. A. Morgan, "THE REDUCTION BY ONE OF THE NUMBER OF INDEPENDENT VARIABLES IN SOME SYSTEMS OF PARTIAL DIFFERENTIAL EQUATIONS," Q J Math The Quarterly Journal of Mathematics, vol. 3, pp. 250-259, 1952.
[34] M. Sheikholeslami, "Effect of uniform suction on nanofluid flow and heat transfer over a cylinder," Journal of the Brazilian Society of Mechanical Sciences and Engineering, vol. 37, pp. 1623-1633, 2015/11/01 2015.
[35] M. Sheikholeslami and D. D. Ganji, "Effect of adding nanoparticle on squeezing flow and heat transfer improvement using KKL model," International Journal of Numerical Methods for Heat & Fluid Flow, vol. 27, pp. 1535-1553, 2017.
[36] M. Mahmoodi and S. Kandelousi, "Cooling process of liquid propellant rocket by means of kerosene-alumina nanofluid," Propulsion and Power Research, vol. 5, pp. 279-286, 2016/12/01/ 2016.
[37] A. Khan, D. Khan, I. Khan, F. Ali, F. u. Karim, and M. Imran, "MHD Flow of Sodium Alginate-Based Casson Type Nanofluid Passing Through A Porous Medium With Newtonian Heating," Scientific Reports, vol. 8, p. 8645, 2018/06/05 2018.
[38] C. Yin, L. Zheng, C. Zhang, and X. Zhang, "Flow and heat transfer of nanofluids over a rotating disk with uniform stretching rate in the radial direction," Propulsion and Power Research, vol. 6, pp. 25-30, 2017/03/01/ 2017.
[39] H. R. Ashorynejad, M. Sheikholeslami, I. Pop, and D. D. Ganji, "Nanofluid flow and heat transfer due to a stretching cylinder in the presence of magnetic field," Heat Mass Transfer Heat and Mass Transfer, vol. 49, pp. 427-436, 2013.